

Standardization of ^{123}I -*meta*-iodobenzylguanidine myocardial sympathetic activity imaging: phantom calibration and clinical applications

Kenichi Nakajima¹ · Derk O. Verschure^{2,3} · Koichi Okuda⁴ · Hein J. Verberne²

Received: 10 March 2017 / Accepted: 19 April 2017 / Published online: 4 May 2017
© The Author(s) 2017. This article is an open access publication

Abstract

Purpose Myocardial sympathetic imaging with ^{123}I -*meta*-iodobenzylguanidine (^{123}I -*m*IBG) has gained clinical momentum. Although the need for standardization of ^{123}I -*m*IBG myocardial uptake has been recognized, the availability of practical clinical standardization approaches is limited. The need for standardization includes the heart-to-mediastinum ratio (HMR) and washout rate with planar imaging, and myocardial defect scoring with single-photon emission computed tomography (SPECT).

Methods The planar HMR shows considerable variation due to differences in collimator design. These camera-collimator differences can be overcome by cross-calibration phantom experiments. The principles of these cross-calibration phantom experiments are summarized in this article. ^{123}I -*m*IBG SPECT databases were compiled by Japanese Society of Nuclear Medicine working group. Literature was searched based on the words “ ^{123}I -*m*IBG quantification method”, “standardization”, “heart-to-mediastinum ratio”, and its application to “risk model”.

Results Calibration phantom experiments have been successfully performed in Japan and Europe. The benefit of these cross-calibration phantom experiments is that

variation in the HMR between institutions is minimized including low-energy, low-medium-energy and medium-energy collimators. The use of myocardial ^{123}I -*m*IBG SPECT can be standardized using ^{123}I -*m*IBG normal databases as a basis for quantitative evaluation. This standardization method can be applied in cardiac event prediction models.

Conclusion Standardization of myocardial ^{123}I -*m*IBG outcome parameters may facilitate a universal implementation of myocardial ^{123}I -*m*IBG scintigraphy.

Keywords Quantification · Heart-to-mediastinum ratio · Calibration phantom · Conversion coefficient · Collimator

Introduction

Heart failure (HF) is a life-threatening disease affecting approximately 26 million people worldwide [1]. The cardiac sympathetic system is an important neurohormonal compensation mechanism in the pathogenesis of chronic heart failure (CHF). Patients with CHF have increased cardiac sympathetic activity with increased exocytosis of norepinephrine (NE) from the presynaptic vesicles and impaired NE re-uptake via the norepinephrine transporter in the sympathetic terminal nerve axons. This results in increased NE levels in the synaptic cleft. Initially, β -adrenergic receptor stimulation by increased synaptic NE levels helps to compensate for impaired myocardial function. However, long-term NE excess has detrimental effects on myocardial structure and gives rise to a down-regulation and availability of post-synaptic β -adrenergic receptor. This leads to left ventricular remodeling and is associated with increased mortality and morbidity in CHF. CHF presents high mortality rates and around 50% of

✉ Kenichi Nakajima
nakajima@med.kanazawa-u.ac.jp

¹ Department of Nuclear Medicine, Kanazawa University, 13-1 Takara-machi, Kanazawa 920-8641, Japan

² Department of Nuclear Medicine, Academic Medical Center, University of Amsterdam, Amsterdam, The Netherlands

³ Department of Cardiology, Zaans Medical Center, Zaandam, The Netherlands

⁴ Department of Physics, Kanazawa Medical University, Uchinada, Kahoku, Japan

deaths are related to sudden death. The European data (ESC-HF pilot study) demonstrate that 12-month all-cause mortality rates for hospitalized and stable/ambulatory CHF patients were 17 and 7%, respectively [2]. The majority of these deaths are caused by progression of HF, lethal arrhythmia and sudden cardiac death.

Myocardial ^{123}I -meta-iodobenzylguanidine (^{123}I -mIBG) scintigraphy has the unique characteristic of reflecting myocardial sympathetic activity and has been used in treating many kinds of cardiac diseases [3–6]. In particular, in patients with CHF, myocardial ^{123}I -mIBG scintigraphy is the most common indication in Japan, Europe and the United States [7, 8]. However, myocardial ^{123}I -mIBG is also widely used for the diagnosis of Lewy body-related disorders [9, 10], and recently the number of ^{123}I -mIBG studies for neurological indications has exceeded cardiac applications in Japan [11]. While various quantitation methods for measuring myocardial uptake have been used, the simplest and most practically used index has been heart-to-mediastinum ratio (HMR) [12]. However, there are inter-institutional variations in HMR, even for normal values. Especially the choice of collimator introduces considerable variations [13, 14]. Therefore, the need for standardization of ^{123}I -mIBG myocardial uptake has been recognized. However, the availability of practical clinical standardization approaches is limited. To overcome this variation and to unify HMRs from various data acquisition systems, a cross-calibration phantom was developed [15, 16]. In this article, the general idea behind this cross-calibration method is reviewed. Literature was searched using the following words: “quantification”, “ ^{123}I -mIBG”, “heart-to-mediastinum ratio”, “washout rate”, “standardization”, “collimators”, and “phantoms”. In addition, the use of this standardization method in cardiac event prediction models is included. Last but not least, standardization methods for myocardial ^{123}I -mIBG single-photon emission computed tomography (SPECT) are discussed.

What should be standardized?

Since the introduction of the HMR in patients with CHF, it has been widely used as a practical method to reflect myocardial sympathetic activity. The need for standardization in ^{123}I -mIBG studies has been recognized for quantitation methods [17–20]. The HMR is a practical but crude parameter and is calculated by an average count ratio between heart and mediastinum. However, the practical simplicity of the HMR does not necessarily result in its uniformity, and various factors are known to cause variations in the HMR [7, 12]. Since the HMR is determined by an averaged count ratio of heart and mediastinum, the location, size, and shape of the region of interest (ROI)

could be a factor of the variations. Although in clinical practice such variations between hospitals exist, the reproducibility of the HMR is generally believed to be good [21, 22]. However, some variations still exist depending on ROI setting methods even around the prognostic threshold of HMR (1.6), and predefined or semiautomatic methods for defining ROI are preferable [22–24]. Another critical factor is related to camera–collimator combinations, in particular, regarding low-energy (LE) and medium-energy (ME) collimators [13–15]. The HMR derived from ME collimators is higher than that from LE collimators. The Japanese Society of Nuclear Medicine working group (JSNM-WG) normal databases showed an average HMR of 2.5 (range of mean \pm 2 standard deviation: 1.9–3.1) and 3.0 (range 2.0–4.3) for the LE and ME collimators, respectively [25]. Although the use of ME collimators is advocated [12], many hospitals still use LE collimators because of limited availability of ME collimators. Moreover, especially in Japan, as the use of ^{123}I -labeled tracers for brain perfusion and myocardial imaging is common, various types of collimators have specifically been designed for these ^{123}I -labeled radiopharmaceuticals. One may argue that calculated HMRs are consistent if all institutions were to use the same type of collimators. However, collimator specifications such as hole diameter, length and septal thickness may significantly differ between manufacturers despite the fact that these collimators have similar names. The impact of these variations in collimators on the HMR is best illustrated by a Japanese multicenter phantom study [16]. In this study variations in the phantom identified an HMR of 1.6 for the same LE high-resolution (LEHR) collimators which ranged in measured values between 1.50 and 1.74 [26].

Structure of the phantom and experiments

To cross-calibrate camera–collimator systems in various hospitals, a calibration phantom was introduced and successfully applied in 225 conditions in Japan [16], and subsequently validated in Europe in 210 conditions [27]. Additionally, as of 2016 nearly 1300 calibration phantom experiments for additional collimators were performed using the same acquisition protocol. The calibration phantom was designed for planar acquisitions for the calculation of the HMR only (Fig. 1). Although it cannot be used for SPECT acquisitions, the design allows for acquiring images from anterior and posterior views resulting in a different HMR. The phantom is made of acrylic with two separate compartments: one compartment can be filled with a ^{123}I solution (111–185 MBq) and the second compartment can be filled with water. Mediastinum, liver, lung and heart are simulated by variation in acrylic thickness

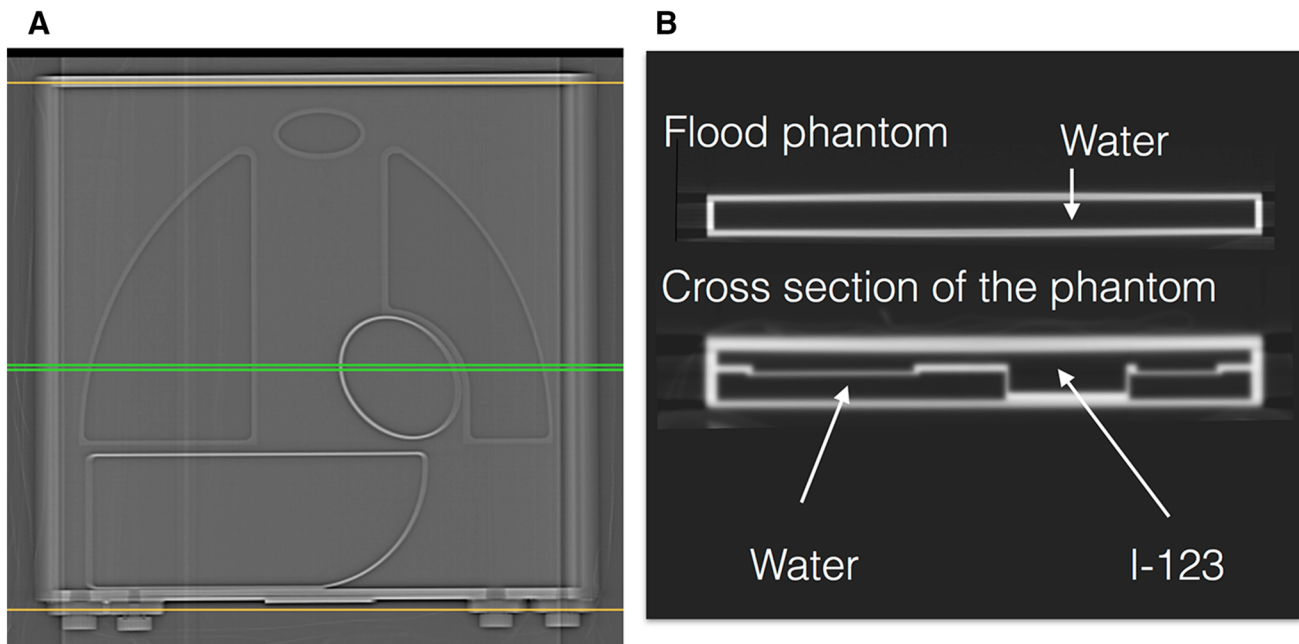


Fig. 1 Cross-calibration phantom with a scout anterior view (a) and transverse X-ray CT cross section (b) illustrating the structure of the phantom and the different simulated organs

that separates the two compartments. As ^{123}I can be distributed homogeneously in one compartment, adjustment for ^{123}I concentrations is not necessary. Both sides of the phantom (i.e., anterior and posterior) can be imaged resulting in a different HMR. Typically the protocol used for the described phantom experiments included a 256×256 matrix and an acquisition duration of 5 min [16, 27]. The energy window was centered at 159 keV with a range of 15–20%.

Conversion coefficient for collimators

In the initial experiments, four phantom types were used, and eight HMRs could be calculated to make a linear regression line between two camera systems [15]. The reference HMR was calculated mathematically using attenuation factors ranging from 1.55 to 4.48 (Fig. 2). Thereafter, the number of phantoms was first reduced to two and finally to only one. The reduction of phantoms was based on the fact that the variation in regression lines between different camera systems did not change with the lower number of phantoms, ultimately leading to only one phantom (i.e., with 2 different HMRs) [15]. The slope K was defined as the conversion coefficient (CC) that allows for the conversion of measured values to reference values. This mathematically calculated HMR was used as the reference or gold standard, for which attenuation in the acrylic plates and water was calculated. Although HMRs from any two camera–collimator systems can be cross-

calibrated, we extended the idea to calculate one single standardized condition, so that any institution can calculate HMRs using essentially the same scale. Since the European proposal advocated the use of ME collimators [12], we decided to calibrate all HMRs from any collimators to a ME general-purpose (MEGP) collimator condition. This resulted in a CC of 0.88 (ME88 condition). The conversion equation is as follows:

$$\text{HMR}_{\text{std}} = \left\{ \frac{\text{CC}_{\text{std}}}{\text{CC}_{\text{institution}}} \right\} * (\text{HMR}_{\text{institution}} - 1) + 1,$$

where HMR_{std} is the standardized HMR, CC_{std} is 0.88, $\text{CC}_{\text{institution}}$ is the CC for the specific institutional camera–collimator system, and $\text{HMR}_{\text{institution}}$ is the institutional measured HMR, respectively.

The conversion coefficients measured in Japanese and European studies are summarized in Fig. 3 [16, 27]. There was a good agreement between Japanese and European LE high-resolution (LEHR), low–medium-energy (LME) and MEGP collimators. This finding is most likely a good basis for comparing the data from different camera–collimator systems worldwide. It should be noted that collimator designs are different among companies. Although this variation in CC is smaller for gamma-camera–collimator combinations from the same vendors, differences still exist for the contemporary camera types [27]. This is illustrated by, for example, the extended low-energy general-purpose collimator (GE Healthcare). This collimator showed different CC (0.62 ± 0.03 and 0.75 ± 0.03) depending on camera types used. The differences could be explained by

Fig. 2 Anterior and posterior phantom images obtained with medium-energy low-penetration (MELP) and low-energy high-resolution (LEHR) collimators. Difference in background count due to septal penetration and scatter can be clearly seen

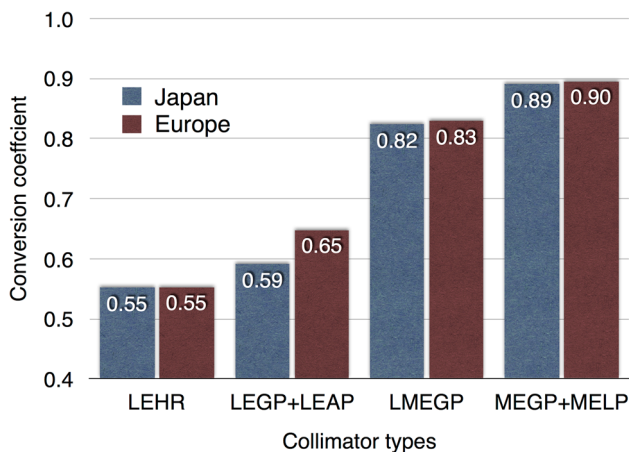
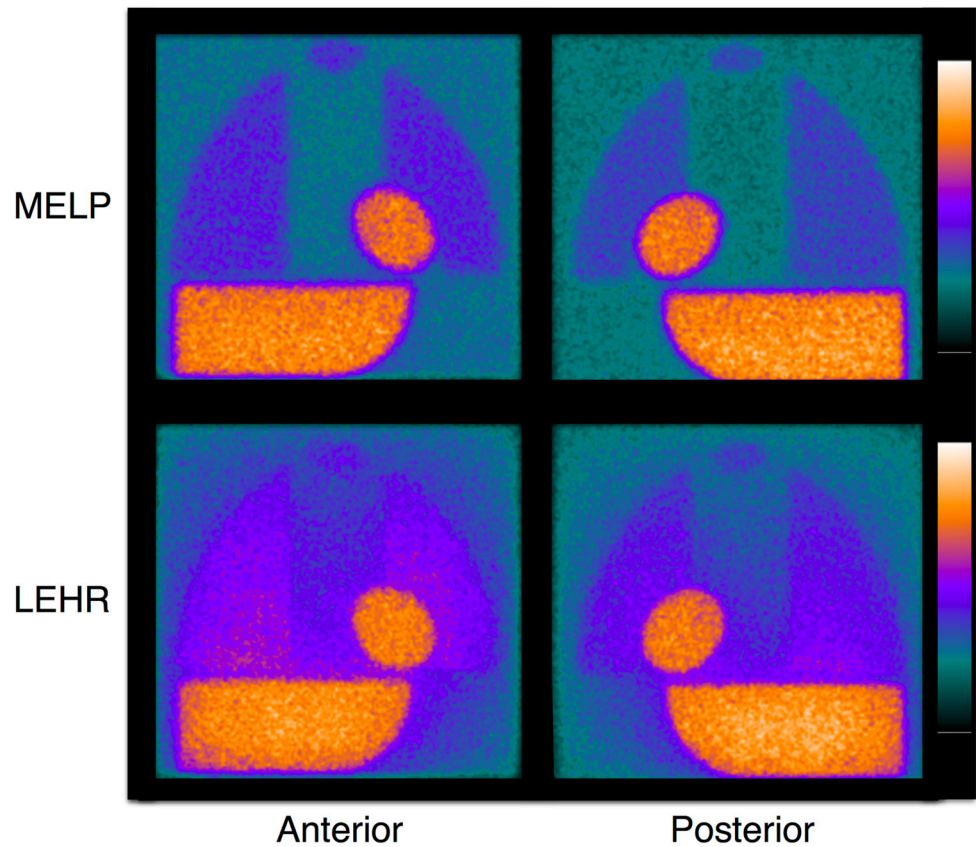


Fig. 3 Conversion coefficients obtained in Japanese and European centers [16, 27]

the fact that collimator specifications were modified while maintaining the same collimator name. Applicability of the camera–collimator-specific CC should be further validated in the United States.

Using the CC of the ME88 condition, average and normal range of HMR including both ME and LE collimators

became 3.1 (range 2.2–4.0) for early HMR and 3.3 (range 2.2–4.4) for late HMR in JSNM-WG databases [28].

In addition to the phantom-based approach as shown in this article, several methods have been described to correct for differences between collimators. Multiple energy window methods including triple energy window and dual-energy window methods were used to subtract scatter or penetration fraction [15, 29–31]. These corrections did not completely compensate the error in calculation. Empiric correction between two camera systems could be used in a single center [32], but this approach is limited by the need for additional experiments in other camera–collimator combinations. Chen et al. used ^{123}I cardiac SPECT imaging with deconvolution of septal penetration, and significantly improved quantitation in ^{123}I cardiac SPECT imaging [33]. They also applied three-dimensional SPECT approach for calculating HMR [34]. However, from a prognostic point of view, HMR obtained from SPECT was equivalent to the planar HMR for differentiating between subjects with normal and abnormal ^{123}I -mIBG uptake. Compared to these methods, a phantom-based correction is practical and applicable for any camera–collimator combination. The HMR provided by a specific collimator type in one hospital can be adjusted to any other camera–collimator conditions.

Washout rate

The ^{123}I -*m*IBG washout rate (WR) is considered to reflect sympathetic drive in physiological and pathological conditions. It has thus been recognized as a predictor of cardiac events and more specifically as a predictor of sudden cardiac death. WR (%) is defined as:

$$\text{WR} = \left\{ \frac{(\text{early H} - \text{early M}) - (\text{late H} - \text{late M}) * \text{decay correction factor}}{(\text{early H} - \text{early M})} \right\} * 100\%$$

where decay correction factor = $1/0.5^{\text{(time between early and late imaging (h)/13)}}$ [12] (asterisk denotes multiplication). In this formula, depending on the use of background subtraction and decay correction, four possible calculation methods can be used, but applications of both time decay and background corrections are generally recommended. In addition, the duration between early and late imaging varies from 2.5 to 5 h in clinical practice, and the definition of WR varies considerably between studies. These potential factors that influence the WR should be standardized, and where possible, correction to a reference value is required [11, 12]. Despite the differences in the time between the late and early acquisition, a correction method for WR may be feasible.

Compared to WR, the late HMR is relatively consistent in CHF patients from 2 to 4 h after the administration of ^{123}I -*m*IBG [35, 36], and even a single early-only imaging may be used particularly in patients with Lewy body disease [37]. To obtain reproducible results, caution is required when myocardial uptake is very low. After subtraction of background, the denominator of the above-mentioned equation becomes small, and fluctuation of WR becomes larger. Therefore, the WR should be carefully checked in CHF patients and in patients with Lewy body disease with low myocardial ^{123}I -*m*IBG uptake.

Another definition of WR used the following equation: $\text{WR} (\%) = (\text{early HMR} - \text{late HMR}) / \text{early HMR} * 100$ [38–40] (asterisk denotes multiplication). The WR calculated with this definition is influenced by the standardization to the ME88 condition.

Myocardial ^{123}I -*m*IBG SPECT

Defect scoring has been successfully used for myocardial perfusion imaging. The aim of scoring is not only for diagnostic purposes but also to guide therapeutic decision-making. Similar to perfusion studies, the extent and severity of ^{123}I -*m*IBG SPECT images can be semi-quantitatively scored. This can be done by a simple visual analysis of the

innervation images alone. However, by combining perfusion and innervation images, additional information can be obtained [41]. In most patients with ischemic heart failure, innervation defects are more pronounced than perfusion defects, and the size of mismatch or perfusion–innervation imbalance seems to correlate with the occurrence of serious ventricular arrhythmias [42]. Inhomogeneity of regional sympathetic denervation may be related to serious arrhythmic events and sudden cardiac death. Interestingly, regional myocardial denervation instead of global ^{123}I -*m*IBG myocardial uptake was an independent predictor of a positive outcome of electrophysiological studies [43, 44]. To perform this sort of semi-quantitative analysis, normal ^{123}I -*m*IBG databases are desirable as a basis for quantitative evaluations. These databases will help us to better understand normal variations in myocardial ^{123}I -*m*IBG distribution. For example a decreased uptake in the inferior wall is sometimes observed, particularly in elderly patients. Figure 4 shows polar plots based on the normal databases from the Japanese Society of Nuclear Medicine working group [43]. Mid to apical inferior walls show relatively low counts, particularly in male subjects with 180-degree rotation acquisition. It is also noteworthy that the apical inferior segments on the deviation maps show larger deviation compared with other segments. Based on these normal databases, slightly decreased activity in the inferior regions is not judged as abnormal. These normal databases can help us to define physiological variations during interpretation.

Mortality risk models

Standardization of the ^{123}I -*m*IBG HMR is especially important in estimating prognosis. After the publication of the ADMIRE-HF study, a HMR cut-off value of 1.6 has often been used for clinical studies in CHF. In this multi-center study, all hospitals used LEHR collimators from several vendors. This cut-off value of 1.6 should be interpreted differently depending on institutional camera–collimator types. As the HMRs for various collimator types are linearly converted versus CC, corresponding HMR values of $\text{HMR} = 1.6$ for the LEHR collimator versus CC are shown in Fig. 5.

More importantly, the risk of cardiac death is multi-factorial, including age, sex, NYHA functional class, left ventricular ejection fraction (LVEF), B-type natriuretic peptide (BNP), and the late ^{123}I -*m*IBG HMR [25]. Among these various parameters, we have selected 5 prognostic variables, including the late ^{123}I -*m*IBG HMR, and successfully made risk models [45, 46] (Fig. 6). To apply such risk models, HMRs from different acquisition conditions should be standardized so that reliable calculations can be performed.

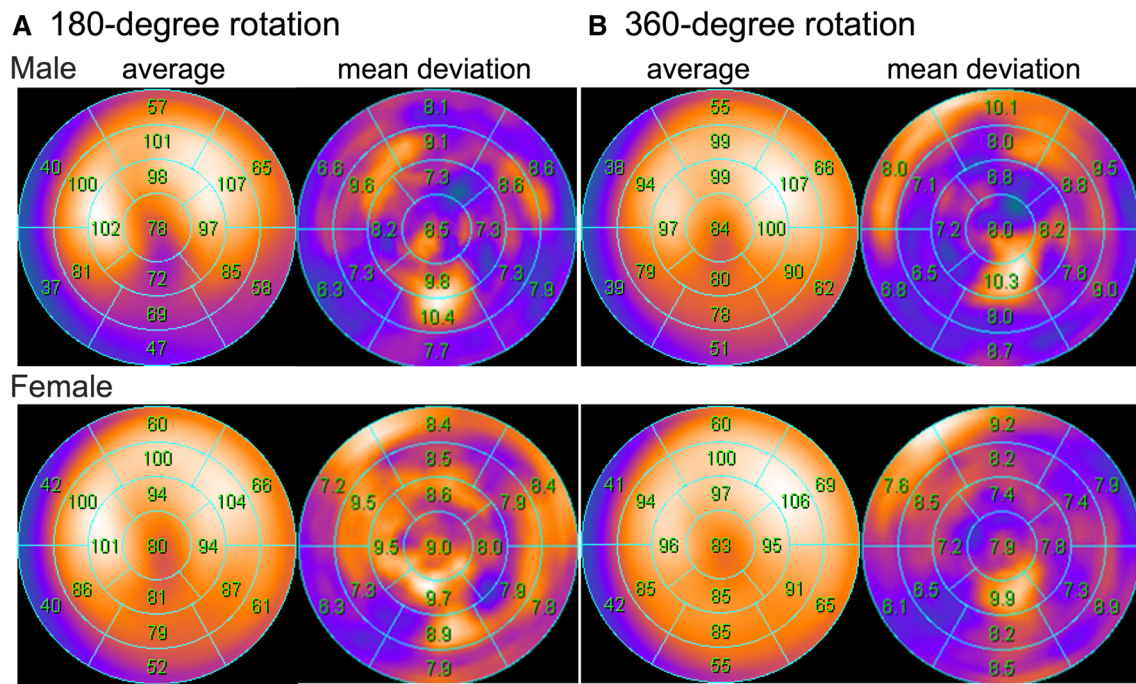


Fig. 4 Normal polar plots of the late phase (3–4 h) SPECT ^{123}I -mIBG images based on the normal ^{123}I -mIBG databases from the Japanese Society of Nuclear Medicine working group [25, 28]

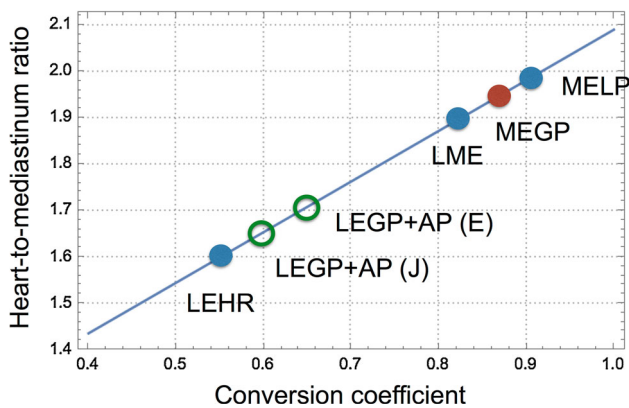


Fig. 5 Relationship between heart-to-mediastinum ratio (HMR) and conversion coefficient (CC) using the HMR threshold of 1.6. For example, HMR = 1.6 with a LEHR collimator (CC = 0.55) can be interpreted as 1.9 with the LME collimator (CC = 0.83). Low-energy general-purpose (LEGP) + all-purpose (AP) groups show variable results between Japan (J) and Europe (E). See also average CC in Fig. 3

Application of standardized HMR in the literature

A number of studies have been performed in cardiology and neurology using the ^{123}I -mIBG HMR. Although meta-analyses and comparative studies have been performed, standardization is useful to integrate results from various studies. As mentioned previously, averaged HMRs in normal subjects are 2.5 for LEHR collimators and 3.0 for MEGP collimators. Looking at HMR normal values in various Japanese studies from 1994 to 2007, the mean early

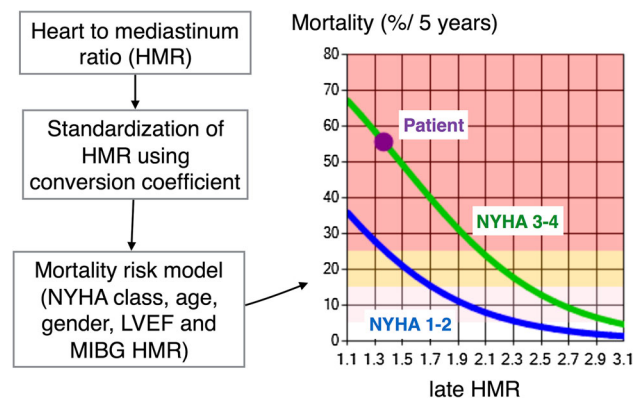


Fig. 6 Application of the heart-to-mediastinum ratio (HMR) in a risk model. A sample plot of 5-year cardiac mortality risk is shown in a 54-year-old man with chronic heart failure, which is expressed as a function of HMR. This calculation is based on conditions of NYHA class III, left ventricular ejection fraction of 20%, and HMR of 1.4, and estimated mortality is 56%/5 years (purple dot) [45, 46]

and late HMRs in the control groups ranged from 1.88 to 2.87 and from 1.84 to 2.49, respectively [45, 46]. In patients with CHF, the best thresholds for differentiating good and bad prognosis and Lewy body and non-Lewy body diseases ranged from 1.5 to 2.1. If the original databases can be accessed with information from the camera-collimator system used, individual HMR data can be corrected. This most likely will reduce the observed variation between the different studies. Even when we compare individual institutional data to the published data, such

cross-calibration can be done, and approximate values fitted for individual camera–collimator conditions can be calculated.

Standardization: perspectives

Ideally, all institutions using myocardial ^{123}I -*m*IBG scintigraphy should have their acquisition machines cross-calibrated. This would result in universally applicable cut-off values. In addition, this would result in more uniform risk models. This cross-calibration process will take time. Therefore, it is essential that the currently available data on myocardial ^{123}I -*m*IBG scintigraphy of published studies should undergo some form of correction. Ultimately this will make these data easier to implement in clinical practice and will allow for more reliable risk models.

Conclusion

In CHF, cardiac ^{123}I -*m*IBG scintigraphy alone and more likely in combination with other determinants may be able to better select CHF patients with increased risk. Standardization of myocardial ^{123}I -*m*IBG outcome parameters is, therefore, essential. This standardization may facilitate a universal implementation of myocardial ^{123}I -*m*IBG scintigraphy. The use of a cross-calibration phantom is an effective method for comparing and compiling multicenter databases. In addition, these cross-calibrated HMRs allow for adequate risk models. The role of myocardial ^{123}I -*m*IBG scintigraphy in cardiac and neurological applications should be re-evaluated based on such standardized approaches.

Acknowledgements The authors appreciate the collaboration of medical doctors and technologists who participated in multicenter studies in Japan and Europe. The phantom experimental studies are partly supported by JSPS Grants-in-Aid for Scientific Research (C) in Japan (No. 15K09947, PI: K. Nakajima), FUJIFILM RI Pharma Co. Ltd, and GE healthcare B.V. (Grant Number ADR-14-03). Participated hospitals are listed in references 14 and 17. Authors thank Mr. Ronald Belisle for editorial assistance.

Author contribution statement KN: content planning, literature search, manuscript writing. DV: literature search, manuscript editing, and database collection. KO: literature search, manuscript editing, and database collection. HV: content planning, manuscript writing and editing.

Compliance with ethical standards

Conflict of interest K. Nakajima and K. Okuda have collaborative works to develop software with FUJIFILM RI Pharma, Co. Ltd, Tokyo, Japan.

Ethical approval and informed consent Ethical approval and informed consent statements were shown in individual studies in references.

Open Access This article is distributed under the terms of the Creative Commons Attribution 4.0 International License (<http://creativecommons.org/licenses/by/4.0/>), which permits unrestricted use, distribution, and reproduction in any medium, provided you give appropriate credit to the original author(s) and the source, provide a link to the Creative Commons license, and indicate if changes were made.

References

- Bui AL, Horwich TB, Fonarow GC (2011) Epidemiology and risk profile of heart failure. *Nat Rev Cardiol* 8:30–41
- Maggioni AP, Dahlstrom U, Filippatos G, Chioncel O, Crespo Leiro M, Drozd J et al (2013) EURObservational Research Programme: regional differences and 1-year follow-up results of the Heart Failure Pilot Survey (ESC-HF Pilot). *Eur J Heart Fail* 15:808–817
- Agostini D, Verberne HJ, Burchert W, Knuuti J, Povinec P, Sambuceti G et al (2008) I-123-*m*IBG myocardial imaging for assessment of risk for a major cardiac event in heart failure patients: insights from a retrospective European multicenter study. *Eur J Nucl Med Mol Imaging* 35:535–546
- Jacobson AF, Senior R, Cerqueira MD, Wong ND, Thomas GS, Lopez VA et al (2010) Myocardial iodine-123 meta-iodobenzylguanidine imaging and cardiac events in heart failure. Results of the prospective ADMIRE-HF (AdreView Myocardial Imaging for Risk Evaluation in Heart Failure) study. *J Am Coll Cardiol* 55:2212–2221
- Nakata T, Nakajima K, Yamashina S, Yamada T, Momose M, Kasama S et al (2013) A pooled analysis of multicenter cohort studies of ^{123}I -*m*IBG imaging of sympathetic innervation for assessment of long-term prognosis in heart failure. *JACC Cardiovasc Imaging* 6:772–784
- Verschure DO, Veltman CE, Manrique A, Somsen GA, Koutelou M, Katsikis A et al (2014) For what endpoint does myocardial ^{123}I -MIBG scintigraphy have the greatest prognostic value in patients with chronic heart failure? Results of a pooled individual patient data meta-analysis. *Eur Heart J Cardiovasc Imaging* 15:996–1003
- Henzlova MJ, Duvall WL, Einstein AJ, Travin MI, Verberne HJ (2016) ASNC imaging guidelines for SPECT nuclear cardiology procedures: stress, protocols, and tracers. *J Nucl Cardiol* 23:606–639
- JCS Joint Working Group (2010) Guidelines for clinical use of cardiac nuclear medicine (Japanese Circulation Society 2010). https://www.jstage.jst.go.jp/article/circj/76/3/76_CJ-88-0019/_pdf. Accessed 27 Apr 2017 (**English digest version**)
- Treglia G, Cason E (2012) Diagnostic performance of myocardial innervation imaging using MIBG scintigraphy in differential diagnosis between dementia with Lewy bodies and other dementias: a systematic review and a meta-analysis. *J Neuroimaging* 22:111–117
- King AE, Mintz J, Royall DR (2011) Meta-analysis of ^{123}I -MIBG cardiac scintigraphy for the diagnosis of Lewy body-related disorders. *Mov Disord* 26:1218–1224
- Nakajima K, Nakata T (2015) Cardiac ^{123}I -MIBG Imaging for clinical decision making: 22-year experience in Japan. *J Nucl Med* 56(Suppl 4):11S–19S
- Flotats A, Carrio I, Agostini D, Le Guludec D, Marcassa C, Schafers M et al (2010) Proposal for standardization of ^{123}I -

- metaiodobenzylguanidine (MIBG) cardiac sympathetic imaging by the EANM Cardiovascular Committee and the European Council of Nuclear Cardiology. *Eur J Nucl Med Mol Imaging* 37:1802–1812
13. Verberne HJ, Feenstra C, de Jong WM, Somsen GA, van Eck-Smit BL, Busemann Sokole E (2005) Influence of collimator choice and simulated clinical conditions on ^{123}I -MIBG heart/mediastinum ratios: a phantom study. *Eur J Nucl Med Mol Imaging* 32:1100–1107
 14. Verschure DO, de Wit TC, Bongers V, Hagen PJ, Sonneck-Koenne C, D'Aron J et al (2015) ^{123}I -MIBG heart-to-mediastinum ratio is influenced by high-energy photon penetration of collimator septa from liver and lung activity. *Nucl Med Commun* 36:279–285
 15. Nakajima K, Matsubara K, Ishikawa T, Motomura N, Maeda R, Akhter N et al (2007) Correction of iodine-123-labeled metaiodobenzylguanidine uptake with multi-window methods for standardization of the heart-to-mediastinum ratio. *J Nucl Cardiol* 14:843–851
 16. Nakajima K, Okuda K, Yoshimura M, Matsuo S, Wakabayashi H, Imanishi Y et al (2014) Multicenter cross-calibration of I-123 metaiodobenzylguanidine heart-to-mediastinum ratios to overcome camera-collimator variations. *J Nucl Cardiol* 21:970–978
 17. Chen W, Cao Q, Dilsizian V (2011) Variation of heart-to-mediastinal ratio in (123)I-MIBG cardiac sympathetic imaging: its affecting factors and potential corrections. *Curr Cardiol Rep* 13:132–137
 18. Yamashina S, Yamazaki J (2004) Role of MIBG myocardial scintigraphy in the assessment of heart failure: the need to establish evidence. *Eur J Nucl Med Mol Imaging* 31:1353–1355
 19. Verberne HJ, Habraken JB, van Eck-Smit BL, Agostini D, Jacobson AF (2008) Variations in ^{123}I -metaiodobenzylguanidine (MIBG) late heart mediastinal ratios in chronic heart failure: a need for standardisation and validation. *Eur J Nucl Med Mol Imaging* 35:547–553
 20. Pellegrino T, Piscopo V, Petretta M, Cuocolo A (2015) ^{123}I -Metaiodobenzylguanidine cardiac innervation imaging: methods and interpretation. *Clin Transl Imaging* 3:357–363
 21. Veltman CE, Boogers MJ, Meinardi JE, Al Younis I, Dibbets-Schneider P, Van der Wall EE et al (2012) Reproducibility of planar ^{123}I -meta-iodobenzylguanidine (MIBG) myocardial scintigraphy in patients with heart failure. *Eur J Nucl Med Mol Imaging* 39:1599–1608
 22. Verschure DO, Bongers V, Hagen PJ, Somsen GA, van Eck-Smit BL, Verberne HJ (2014) Impact of a predefined mediastinal ROI on inter-observer variability of planar ^{123}I -MIBG heart-to-mediastinum ratio. *J Nucl Cardiol* 21:605–613
 23. Klene C, Jungen C, Okuda K, Kobayashi Y, Helberg A, Mester J et al (2016) Influence of ROI definition on the heart-to-mediastinum ratio in planar ^{123}I -MIBG imaging. *J Nucl Cardiol*. doi:10.1007/s12350-016-0708-8
 24. Okuda K, Nakajima K, Hosoya T, Ishikawa T, Konishi T, Matsubara K et al (2011) Semi-automated algorithm for calculating heart-to-mediastinum ratio in cardiac Iodine-123 MIBG imaging. *J Nucl Cardiol* 18:82–89
 25. Nakajima K (2010) Normal values for nuclear cardiology: Japanese databases for myocardial perfusion, fatty acid and sympathetic imaging and left ventricular function. *Ann Nucl Med* 24:125–135
 26. Slomka PJ, Mehta PK, Germano G, Berman DS (2014) Quantification of I-123-meta-iodobenzylguanidine heart-to-mediastinum ratios: not so simple after all. *J Nucl Cardiol* 21:979–983
 27. Verschure DO, Poel E, Nakajima K, Okuda K, van Eck-Smit BL, Somsen GA et al (2017) A European myocardial ^{123}I -MIBG cross-calibration phantom study. *J Nucl Cardiol*. doi:10.1007/s12350-017-0782-6 (Epub ahead of print)
 28. Nakajima K, Matsumoto N, Kasai T, Matsuo S, Kiso K, Okuda K (2016) Normal values and standardization of parameters in nuclear cardiology: Japanese Society of Nuclear Medicine working group database. *Ann Nucl Med* 30:188–199
 29. Motomura N, Ichihara T, Takayama T, Aoki S, Kubo H, Takeda K (1999) Practical compensation method of downscattered component due to high energy photon in ^{123}I imaging. *Kaku Igaku (Jpn J Nucl Med)* 36:997–1005 (abstract in English)
 30. Fletcher AM, Motherwell DW, Small AD, McCurrach GM, Goodfield NE, Petrie MC et al (2010) I-123 MIBG cardiac uptake measurements: limitations of collimator choice and scatter correction in the clinical context. *Nucl Med Commun* 31:629–636
 31. Inoue Y, Abe Y, Asano Y, Kikuchi K, Matsunaga K, Iizuka T et al (2014) An improved method for estimating the heart-to-mediastinum ratio from cardiac sympathetic nerve imaging with low-energy high-resolution collimators. *J Nucl Cardiol* 21:614–621
 32. Inoue Y, Abe Y, Itoh Y, Asano Y, Kikuchi K, Sakamoto Y et al (2013) Acquisition protocols and correction methods for estimation of the heart-to-mediastinum ratio in ^{123}I -metaiodobenzylguanidine cardiac sympathetic imaging. *J Nucl Med* 54:707–713
 33. Chen J, Garcia EV, Galt JR, Folks RD, Carrio I (2006) Improved quantification in ^{123}I cardiac SPECT imaging with deconvolution of septal penetration. *Nucl Med Commun* 27:551–558
 34. Chen J, Folks RD, Verdes L, Manatunga DN, Jacobson AF, Garcia EV (2012) Quantitative I-123 mIBG SPECT in differentiating abnormal and normal mIBG myocardial uptake. *J Nucl Cardiol* 19:92–99
 35. Okuda K, Nakajima K, Sugino S, Kirihara Y, Matsuo S, Taki J et al (2016) Development and validation of a direct-comparison method for cardiac (123)I-metaiodobenzylguanidine washout rates derived from late 3-hour and 4-hour imaging. *Eur J Nucl Med Mol Imaging* 43:319–325
 36. Dimitriu-Leen AC, Gimelli A, Al Younis I, Veltman CE, Verberne HJ, Wolterbeek R et al (2016) The impact of acquisition time of planar cardiac (123)I-MIBG imaging on the late heart to mediastinum ratio. *Eur J Nucl Med Mol Imaging* 43:326–332
 37. Sakamoto F, Shiraishi S, Tsuda N, Ogasawara K, Yoshida M, Yuki H et al (2016) ^{123}I -MIBG myocardial scintigraphy for the evaluation of Lewy body disease: are delayed images essential? Is visual assessment useful? *Br J Radiol*. doi:10.1259/bjr.20160144
 38. Soman P, Travin MI, Gerson M, Cullom SJ, Thompson R (2015) I-123 MIBG cardiac imaging. *J Nucl Cardiol* 22:677–685
 39. Verschure DO, Baas F, van Eck-Smit BL, Somsen GA, Verberne HJ (2016) Polymorphism of SLC6A2 gene does not influence outcome of myocardial ^{123}I -mIBG scintigraphy in patients with chronic heart failure. *J Nucl Cardiol*. doi:10.1007/s12350-016-0722-x (Epub ahead of print)
 40. Verschure DO, Lutter R, van Eck-Smit BL, Somsen GA, Verberne HJ (2016) Myocardial ^{123}I -MIBG scintigraphy in relation to markers of inflammation and long-term clinical outcome in patients with stable chronic heart failure. *J Nucl Cardiol*. doi:10.1007/s12350-016-0697-7 (Epub ahead of print)
 41. Travin MI, Henzlova MJ, van Eck-Smit BL, Jain D, Carrio I, Folks RD et al (2016) Assessment of I-mIBG and Tc-tetrofosmin single-photon emission computed tomographic images for the prediction of arrhythmic events in patients with ischemic heart failure: Intermediate severity innervation defects are associated with higher arrhythmic risk. *J Nucl Cardiol*. doi:10.1007/s12350-015-0336-8
 42. Scholtens AM, Verberne HJ (2015) Innervation imaging in arrhythmia and arrhythmogenic disease. *Clin Transl Imaging* 3:373–378
 43. Bax JJ, Kraft O, Buxton AE, Fjeld JG, Parizek P, Agostini D et al (2008) ^{123}I -mIBG scintigraphy to predict inducibility of

- ventricular arrhythmias on cardiac electrophysiology testing: a prospective multicenter pilot study. *Circ Cardiovasc Imaging* 1:131–140
44. Zhou Y, Zhou W, Folks RD, Manatunga DN, Jacobson AF, Bax JJ et al (2014) I-123 mIBG and Tc-99m myocardial SPECT imaging to predict inducibility of ventricular arrhythmia on electrophysiology testing: a retrospective analysis. *J Nucl Cardiol* 21:913–920
45. Nakajima K, Nakata T, Yamada T, Yamashina S, Momose M, Kasama S et al (2014) A prediction model for 5-year cardiac mortality in patients with chronic heart failure using ^{123}I -metaiodobenzylguanidine imaging. *Eur J Nucl Med Mol Imaging* 41:1673–1682
46. Nakajima K, Nakata T, Matsuo S, Jacobson AF (2016) Creation of mortality risk charts using ^{123}I meta-iodobenzylguanidine heart-to-mediastinum ratio in patients with heart failure: 2- and 5-year risk models. *Eur Heart J Cardiovasc Imaging* 17:1138–1145